Macromolecules

pubs.acs.org/Macromolecules Article

Onsager Transport Coefficients and Transference Numbers in Polyelectrolyte Solutions and Polymerized Ionic Liquids

Kara D. Fong, Julian Self, Bryan D. McCloskey,* and Kristin A. Persson*

Cite This: https://dx.doi.org/10.1021/acs.macromol.0c02001 Read Online

ACCESS | Metrics & More | Article Recommendations | Supporting Information

ABSTRACT: Electrolytes featuring negatively charged polymers, such as nonaqueous polyelectrolyte solutions and polymerized ionic liquids, are currently under investigation as potential high cation transference number (t_+) electrolytes for lithium-ion batteries. Herein, we use coarse-grained molecular dynamics simulations to characterize the Onsager transport coefficients of polyelectrolyte solutions as a function of chain length and concentration. For all the systems studied, we find that the rigorously computed transference number is substantially lower than that approximated by the ideal solution (Nernst−Einstein) equations typically used to characterize these systems due to the presence of strong anion−anion and cation−anion correlations. None of the polyelectrolyte solutions achieve t_+ greater than that of the conventional binary salt electrolyte, with some solutions having negative t_+. This work demonstrates that the Nernst−Einstein assumption does not provide a physically meaningful estimate of the transference number in these solutions and calls into question the expectation of polyelectrolytes to exhibit a high cation transference number.

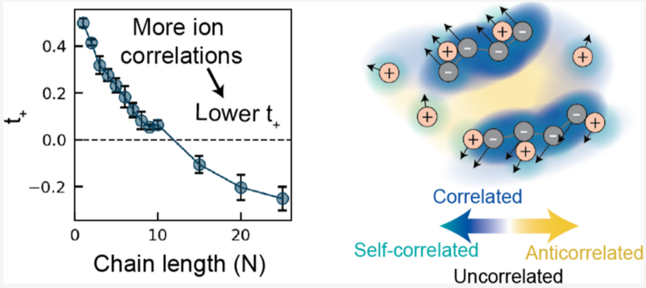

INTRODUCTION

High cation transference number (t_+) electrolytes, in which the majority of the electrolyte conductivity is attributed to the cation rather than the anion, have the potential to improve the power density and attainable state of charge of lithium-ion batteries (LIBs).[1−3] A common strategy in increasing t_+ is to covalently append the electrolyte anion to the backbone of a polymer, thereby immobilizing the anion to yield a single-ion conductor.[4,5] Maintaining acceptable conductivity in a dry (neat) single-ion conducting polymer, however, has proved challenging because of incomplete ion dissociation and/or low ion mobility.[3,6,7]

Polyelectrolyte solutions in which a lithium-neutralized polyanion is dissolved in a nonaqueous solvent have recently been proposed as alternatives to conventional solid-state single-ion conductors.[8−14] As these polyelectrolytes are entirely in the liquid phase, they could serve as a means to increase transference number without drastic conductivity losses and be directly used in existing cell designs. Indeed, initial studies have reported transference numbers greater than 0.8 ($t_+ \sim 0.4$ for conventional LIB electrolytes),[15] with conductivities on the order of 0.1−1 mS/cm.[8,10,11,14] As the transference number is challenging to measure experimentally,[3] the reported t_+ values in these works are typically estimated by assuming that the solution behaves ideally, that is, there are no correlations between the ions in the electrolyte. This is referred to as the Nernst−Einstein (NE) approximation and yields an expression for transference number in terms of the self-diffusion coefficients of the cation and anion, D_+ and D_-, respectively:

$$t_+^{\mathrm{NE}} = \frac{D_+}{D_+ + D_-} \tag{1}$$

While these experimental results seem promising, our previous work[16] on one polyelectrolyte system, poly(allyl glycidyl ether-lithium sulfonate) (PAGELS) in dimethyl sulfoxide (DMSO), found that t_+^{NE} drastically overestimates the true transference number ($t_+^{\mathrm{NE}} \gg t_+$). Using atomistic molecular dynamics simulations, it was shown that the anion−anion correlations inherently present between monomers on the same chain make a substantial contribution to the overall conductivity and therefore decrease the transference number relative to the ideal case.

It remains to be seen, however, whether the failure of eq 1 generalizes beyond the PAGELS system, and whether we can make any more general claims about the extent of nonidealities (ion correlations) in polyelectrolytes which hold independent of the electrolyte chemistry. Furthermore, we wish to understand (i) the emergence of polyelectrolytes' unique

Received: August 31, 2020
Revised: October 4, 2020

transport properties as we transition from a conventional monomeric electrolyte to oligo- and polyanions and (ii) how transport properties change as a function of concentration, including the extreme limit of solvent-free systems or polymerized ionic liquids, which are also under investigation as LIB electrolyte alternatives.[17−21] While existing polyelectrolyte studies have extensively explored the polyion transport properties in these solutions,[22,23] the behavior of the counterion and, thus, the battery-relevant transport properties of polyelectrolytes, such as t_+, are largely unexplored.

Herein, we use coarse-grained molecular dynamics simulations with an explicit solvent to systematically study transport as a function chain length and concentration for a generic polyelectrolyte solution. We begin with an overview of the theoretical framework used to study electrolyte transport. This theory is based on the formulation of transport coefficients, denoted L^{ij}, which provide insights into the ion correlations between species in solution. We then present the transport coefficients computed for the coarse-grained polyelectrolyte model, providing a direct comparison between a conventional binary electrolyte and the polyelectrolyte systems. Next, we use the transport coefficients to calculate the transference number for these solutions, rationalizing the resulting trends based on ion correlations and ion pairing behavior. We find that the strong ion correlations in polyelectrolyte solutions generally yield conductivity and transference number values lower than in monomeric electrolytes, suggesting that—from a transport perspective—polyelectrolytes may not be a promising alternative to conventional battery electrolytes.

■ THEORY

Herein, we analyze transport in electrolytes using the Onsager transport coefficients. The theoretical framework required to define these transport equations is derived and discussed in detail by Fong et al.[24] Here, we summarize only the main components of the theory. The reader may be more familiar with the Stefan−Maxwell equations for multicomponent diffusion, and by extension Newman's concentrated electrolyte theory,[2] rather than the Onsager equations presented in this work. As discussed in Fong et al.,[24] both frameworks are thermodynamically consistent, and it is possible to map between the transport coefficients from the two approaches.[24,25] However, the Onsager transport coefficients L^{ij} have a more direct physical interpretation in terms of ion correlations, and only L^{ij} may be computed directly from molecular simulations using Green−Kubo relations. Furthermore, while it is possible to obtain experimental quantities from the Stefan−Maxwell coefficients K^{ij}, the expressions for doing so are more complex than with L^{ij}, especially for systems with more than two ionic species. These advantages make the Onsager transport equations a clear choice for the analysis in this work. Nevertheless, we provide the Stefan−Maxwell coefficients K^{ij} for the polyelectrolyte solutions studied herein in the Supporting Information for comparison (Figure S6).

The theory of nonequilibrium thermodynamics applied to electrolytes yields the following set of Onsager transport equations:

$$c_i(\boldsymbol{v}_i - \boldsymbol{v}) = -\sum_j L^{ij}\nabla\overline{\mu}_j \tag{2}$$

These equations relate the flux of species i, $\boldsymbol{J}_i = c_i(\boldsymbol{v}_i - \boldsymbol{v})$, to the thermodynamic driving force in the system: gradients in the electrochemical potential of each species j, $\overline{\mu}_j$. In eq 2, c_i and $\boldsymbol{v}_i$ are the concentration and velocity of species i, respectively, and $\boldsymbol{v}$ is the mass-averaged velocity of the entire system. The constants of proportionality in this linear relationship are the transport coefficients L^{ij}. The transport matrix is symmetric by the Onsager reciprocal relations ($L^{ij} = L^{ji}$) and subject to the constraint that $\sum_i M_i L^{ij} = 0$, where M_i is the molecular weight of species i. The latter relation is a consequence of the fact that all mass fluxes must sum to zero, that is, $\sum_i M_i \boldsymbol{J}_i = 0$. Based on these two constraints, an electrolyte of n components has $n(n - 1)/2$ independent transport coefficients. The polyelectrolyte solutions studied herein have three components (polyanion, cation, and solvent), yielding three independent transport coefficients: L^{++}, L^{--}, and L^{+-}.

On a molecular level, L^{ij} may be interpreted as giving the degree of correlation between the motion of species i and j. This is apparent quantitatively from the Green−Kubo relations for L^{ij}, where the correlation function in the fluxes of species i and j gives the transport coefficients directly from molecular simulations:

$$L^{ij} = \frac{V}{3k_BT}\int_0^\infty dt\langle \boldsymbol{J}_i(t)\cdot \boldsymbol{J}_j(0)\rangle \tag{3}$$

where V is the volume and k_BT is the thermal energy. Note that the overall flux of species i, $\boldsymbol{J}_i = c_i(\boldsymbol{v}_i - \boldsymbol{v})$, is based on the average motion of all particles of species i. The quantity $\boldsymbol{v}_i$ can be expressed as $\boldsymbol{v}_i = 1/N_i\sum_\alpha \boldsymbol{v}_i^\alpha$, where the index α refers to an individual particle of type i, and N_i is the number of particles of type i in the system.

The Green−Kubo relations of eq 3 may be equivalently written in terms of particle positions, rather than velocities. This form of the equation, which is analogous to computing self-diffusion coefficients from the mean-squared displacement of particle positions, is the one used to compute L^{ij} in this work:

$$L^{ij} = \frac{1}{6k_BTV}\lim_{t\to\infty}\frac{d}{dt}\left\langle \sum_\alpha [\boldsymbol{r}_i^\alpha(t) - \boldsymbol{r}_i^\alpha(0)]\cdot \sum_\beta [\boldsymbol{r}_j^\beta(t) - \boldsymbol{r}_j^\beta(0)]\right\rangle \tag{4}$$

where $\boldsymbol{r}_i^\alpha$ is the position of particle α relative to the center-of-mass position of the entire system.

Let us further consider the diagonal terms of the transport matrix, L^{ii}:

$$L^{ii} = \frac{1}{6k_BTV}\lim_{t\to\infty}\frac{d}{dt}\sum_\alpha\sum_\beta\langle [\boldsymbol{r}_i^\alpha(t) - \boldsymbol{r}_i^\alpha(0)]\cdot [\boldsymbol{r}_i^\beta(t) - \boldsymbol{r}_i^\beta(0)]\rangle \tag{5}$$

These transport coefficients are composed of two contributions: when $\alpha = \beta$, we take the autocorrelation function of the flux of particle α, and when $\alpha \neq \beta$, we compute the cross-correlations between two distinct particles. These two contributions may be denoted self and distinct terms, respectively:

$$L^{ii}_{\text{self}} = \frac{1}{6k_BTV}\lim_{t\to\infty}\frac{d}{dt}\sum_\alpha\langle [\boldsymbol{r}_i^\alpha(t) - \boldsymbol{r}_i^\alpha(0)]^2\rangle \tag{6}$$

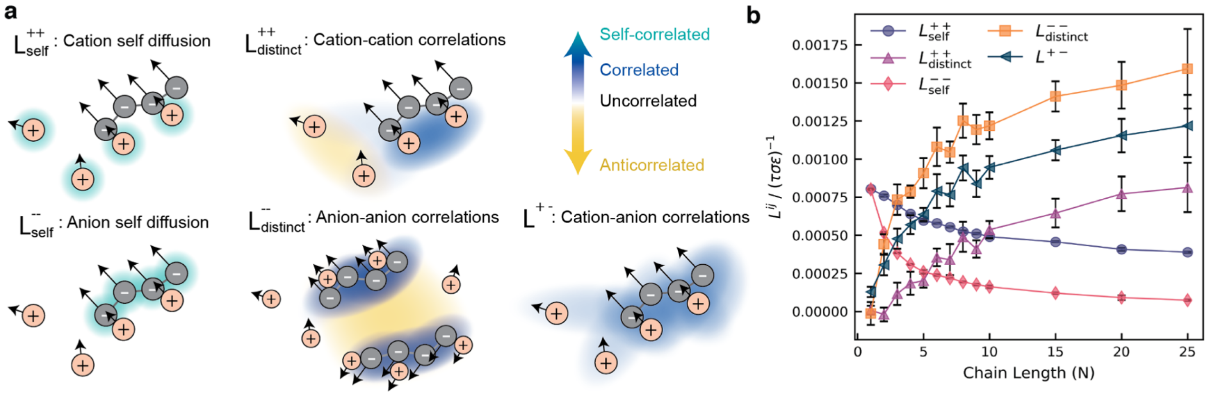

Figure 1. Transport coefficients in polyelectrolyte solutions. (a) Schematics illustrating the ion correlations captured by each transport coefficient. The arrows on each ion indicate direction of motion, and the shaded regions give qualitative information on the correlation between groups of ions according to the color bar in the upper right. Note that solvent molecules are modeled explicitly but are omitted from the schematic for clarity. (b) Each L^{ij} as a function of chain length at a concentration of 0.01 σ^{-3}, split into self- and distinct contributions.

$$L^{ii}_{\text{distinct}} = \frac{1}{6k_{\text{B}}TV}\lim_{t\to\infty}\frac{\text{d}}{\text{d}t}\sum_{\alpha}\sum_{\beta\neq\alpha}\langle[\boldsymbol{r}_i^{\alpha}(t) - \boldsymbol{r}_i^{\alpha}(0)]\cdot [\boldsymbol{r}_i^{\beta}(t) - \boldsymbol{r}_i^{\beta}(0)]\rangle \tag{7}$$

Note that $L^{ii} = L^{ii}_{\text{self}} + L^{ii}_{\text{distinct}}$. The distinct terms capture correlations between particles (nonidealities), while the self-terms may be considered ideal or NE contributions to transport. The latter may be directly related to the self-diffusion coefficient by

$$L^{ii}_{\text{self}} = \frac{D_i c_i}{k_{\text{B}}T} \tag{8}$$

The second law of thermodynamics imposes some restrictions on the possible values of each transport coefficient. While the distinct terms may take on positive or negative values, the self-terms and the overall L^{++} and L^{--} must always be positive. The physical interpretation of each L^{ij} will be discussed in more detail in the Results and Discussion.

The transport coefficients may be combined to yield experimentally relevant transport properties, namely, the ionic conductivity κ, the electrophoretic mobility u_i, and the transference number t_i:

$$\kappa = F^2\sum_i\sum_j L^{ij}z_i z_j \tag{9}$$

$$u_i = \sum_j L^{ij}\frac{z_j F}{c_i} \tag{10}$$

and

$$t_i = \frac{F z_i c_i u_i}{\kappa} = \frac{\sum_j L^{ij}z_i z_j}{\sum_k\sum_l L^{kl}z_k z_l} \tag{11}$$

where F is Faraday's constant and z_i is the charge valence of species i.

The ideal solution transference number, t_i^{NE}, can be computed analogously by assuming that there are no ion correlations, thereby eliminating the off-diagonal components of the transport matrix (L^{+-}) as well as the distinct terms. This yields an expression in terms of only the self-transport coefficients:

$$t_i^{\text{NE}} = \frac{z_i^{\,2}L^{ii}_{\text{self}}}{\sum_j z_j^{\,2}L^{jj}_{\text{self}}} \tag{12}$$

For the cation transference number of a binary electrolyte, incorporating eq 8 and the condition of electroneutrality, $\sum_i z_i c_i = 0$, yields

$$t_+^{\text{NE}} = \frac{z_+D_+}{z_+D_+ - z\_D\_} \tag{13}$$

When computing transport coefficients for a polyelectrolyte system, we may treat either individual monomers or polymer chains as a whole as the anionic species. In the analysis in this work, we choose the former. While this will necessarily impact the transport coefficients, experimentally measurable properties such as the conductivity, mobility, and transference number will be equivalent with either approach (see the Supporting Information for a more detailed discussion). In eq 1, it has implicitly been assumed that $z\_ = -1$, that is, that each monomer is considered to be an independent anionic species.

■ RESULTS AND DISCUSSION

Onsager Transport Coefficients. Here, we present the computed the Onsager transport coefficients for polyelectrolyte solutions using a coarse-grained molecular dynamics model based on the classical Kremer−Grest bead−spring chain[26,27] with an explicit solvent. We simulate chain lengths ranging from 1 to 25, noting that based on previous studies using similar polymer models, we do not expect significant entanglement effects for these chain lengths.[26,28,29] These polyelectrolytes are studied at four concentrations ranging from 0.001 to 0.05 σ^{-3}, where σ is the Lennard-Jones unit of distance and the diameter of each particle in the system. Mapping the size of one monomer bead to that of a polystyrene sulfonate monomer (2.5 Å), this concentration range approximately corresponds to 0.1 to 5 M (see the Methods section for a more detailed discussion).

In this section, we discuss the transport coefficients in these solutions and show how they may be interpreted to gain physical insights into transport phenomena in polyelectrolytes. Each of the transport coefficients L^{ij} quantifies a different aspect of ion motion or ion−ion correlation, illustrated qualitatively in Figure 1a. As a representative example, let us analyze L^{ij} as a function of chain length at a concentration of

https://dx.doi.org/10.1021/acs.macromol.0c02001
Macromolecules XXXX, XXX, XXX−XXX

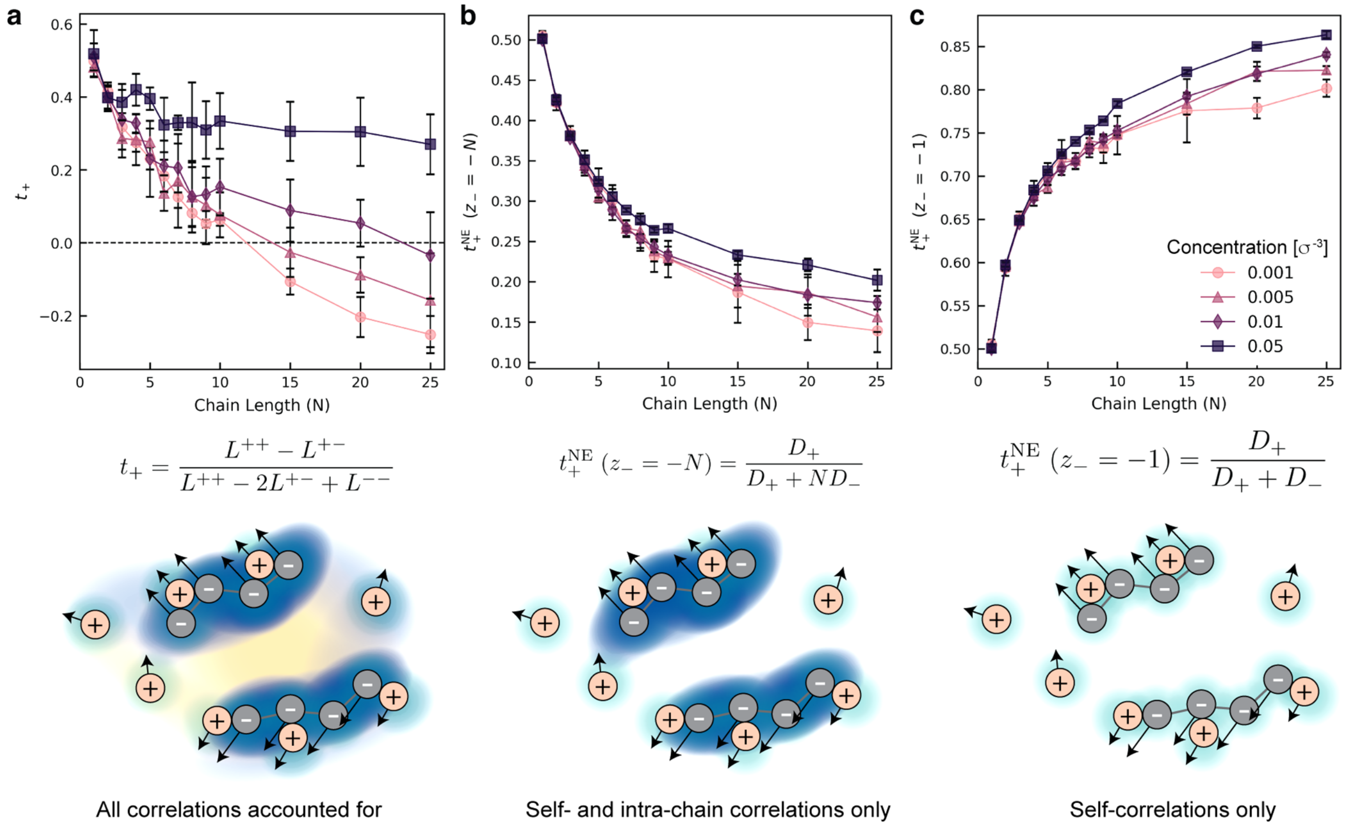

Figure 2. Cation transference number as a function of chain length. (a) Rigorously computed t_+ obtained from the Onsager transport coefficients and accounting for all ion correlations present in solution. (b) and (c) t_+^{NE}, the ideal solution transference number ignoring correlations between ions. These are written in terms of the self-diffusion coefficients, rather than Onsager transport coefficients, using eq 8. (b) Treating entire polymer chains as the anionic species ($z_- = -N$) accounts for intrachain correlations but ignores correlations between chains and between cations and anions. (c) Treating individual monomers as the anionic species ($z_- = -1$) ignores all ionic correlations. Ion correlations are depicted according to the color map in Figure 1.

0.01 σ^{-3}, as shown in Figure 1b. The other concentrations studied give similar trends, as shown in Figures S1 and S2.

The two self-terms (L^{++}_{self} and L^{--}_{self}), as shown in Figure 1b, are proportional to the self-diffusion coefficients (eq 8; diffusion coefficient data are given directly in Figure S8). For the monomeric systems ($N = 1$) corresponding to conventional binary electrolytes, L^{++}_{self} is necessarily equal to L^{--}_{self}, as the cation and anion in the model are equivalent in their mass, size, and excluded volume (Lennard-Jones) interactions. As N increases, both L^{++}_{self} and L^{--}_{self} decrease, a trend which aligns with the intuitive expectation of diffusion coefficients to decrease as the chain becomes larger and the overall solution more viscous. The decrease in L^{--}_{self} is more pronounced because of the bulky nature of the polymer chain.

The L^{+-} transport coefficient captures correlations between cations and anions. The value of L^{+-} is much lower than that of either L^{++} or L^{--} for the $N = 1$ system but becomes increasingly significant as chain length increases. This trend suggests an increased prevalence of ion pairing at higher N, as expected from theories for counterion condensation in polyelectrolytes[30] and confirmed directly in these simulations *vide infra*. Note that when computing ionic conductivity via eq 9, the L^{+-} term will be subtracted from the total value. Thus, as expected, cation−anion correlations decrease the overall conductivity.

Let us now turn to the distinct terms, $L^{++}_{\mathrm{distinct}}$ and $L^{--}_{\mathrm{distinct}}$, which describe cation−cation and anion−anion correlations, respectively. In general, one would expect distinct ions of the same species to interact very little, in which case the distinct terms would be approximately zero, or to repel, leading to negative values of the distinct terms reflecting anticorrelated motion. Indeed, the monomeric ($N = 1$) systems studied here show very small contributions of $L^{++}_{\mathrm{distinct}}$ and $L^{--}_{\mathrm{distinct}}$, with the values at high concentration being slightly negative (Figure S2d). As the chain length increases, however, we deviate from this expected behavior and observe that $L^{++}_{\mathrm{distinct}}$ and $L^{--}_{\mathrm{distinct}}$ increase with chain length. These very positive values suggest highly correlated motion, that is, groups of like-charge ions moving together for appreciable periods of time. Like the trend in L^{+-}, this behavior can be rationalized by increased ion aggregation. The increase of $L^{++}_{\mathrm{distinct}}$ with chain length reflects the presence of multiple cations bound to the same chain, which will move together for the lifetime of the ion aggregate. As the chain length increases (and with it the extent ion pairing), we expect more cations on average to be bound to a given chain, resulting in an increase in the correlations between distinct cations. The increase in $L^{--}_{\mathrm{distinct}}$ with chain length is even more pronounced: for most chain lengths, this term dominates over all other transport coefficients and will thus strongly impact conductivity and transference number. The total value of $L^{--}_{\mathrm{distinct}}$ contains contributions from correlations between anions tethered to the same chain as well as anions on different chains. The former will generate a positive contribution to $L^{--}_{\mathrm{distinct}}$, as anions on a given chain are constrained to move together and are thus highly correlated, while the latter will give a negative contribution, as two negatively charged macroions will repel each other and move in an anticorrelated manner. In all systems studied, we observe that intrachain correlations dominate over interchain correlations (Figure S5), yielding the strong positive trend in $L_{\mathrm{distinct}}^{--}$ with the chain length.

Transference Numbers. Having computed the transport coefficients for a range of polyelectrolyte solutions, we may now combine these L^{ij} to obtain experimentally relevant quantities. Of particular interest is the cation transference number, as shown in Figure 2a; other experimentally relevant quantities such as the conductivity, mobility, and ionicity (inverse Haven ratio) are provided in the Supporting Information. We observe that for all concentrations studied, the transference number decreases as the chain length increases, with the monomeric electrolyte having the highest transference number. Given that ionic conductivity generally decreases as the chain length increases (Figure S7), these results suggest that the polyelectrolyte solutions studied herein would not yield any advantages in battery performance relative to a conventional monomeric electrolyte.

The values of the rigorously computed t_+ stand in stark contrast with the ideal solution transference number, t_+^{NE}. Recall from eq 13 that there are two options for computing t_+^{NE}: we may choose to treat each monomer as a separate ion, in which case z_- appearing in eq 13 is -1, or we may treat the entire polymer chain as the anionic species, in which case $z_- = -N$. The resulting t_+^{NE} values based on each of these choices are given in Figure 2b,c. We observe that t_+^{NE} $(z_- = -N)$ qualitatively reproduces the trend that the transference number decreases as the chain length increases, but in most cases, it overestimates the rigorously computed t_+. This equation ignores correlations between different chains and between cations and anions, but it captures intrachain correlations by treating the entire chain as a single unit. In contrast, t_+^{NE} $(z_- = -1)$ does not account for any correlations between ions, capturing only self-diffusion. This assumes that monomers on the same chain move completely independently, which is obviously incorrect given the fact that they are covalently bonded. The resulting values for t_+^{NE} $(z_- = -1)$, as shown in Figure 2c, increase with chain length, reaching values as high as 0.86. This approximation drastically overestimates the true t_+ and clearly does not provide a physically meaningful estimate of the transference number in polyelectrolytes. In experimental systems where the transference number cannot be rigorously measured and only self-diffusion coefficients are available, t_+^{NE} $(z_- = -N)$ provides a much more reasonable estimate of t_+.

We now seek to rationalize the transference number trends shown in Figure 2 based on the ion correlations in the electrolyte. While each of the L^{ij} affect the observed trends in the transference number, the general decrease in t_+ with increasing chain length can be most directly understood through the trends in L_{self}^{--} and $L_{\mathrm{distinct}}^{--}$, which are shown in Figure 3a. The data in this figure are divided by the total concentration to yield the contribution to each transport coefficient per ion; each of the other transport coefficients is plotted in this manner in Figure S3. For each concentration, the L_{self}^{--} term (and thus the self-diffusion coefficient) decreases with N. Indeed, the fact that a long polymer chain moves more slowly than a monomer is the basis for the intuitive notion that the anion in a polyelectrolyte solution should carry less current than the cation to yield a high t_+. As eq 13 for t_+^{NE} includes only the self-terms (assuming all distinct terms to be zero), it is clear why t_+^{NE} $(z_- = -1)$, as shown in Figure 2c, exhibits such high values. In polyelectrolyte systems, however, it is unreasonable to ignore the distinct terms when estimating t_+, as we observe that the magnitude of $L_{\mathrm{distinct}}^{--}$ surpasses that of L_{self}^{--} for all but the shortest chain lengths. As mentioned above, this increase in $L_{\mathrm{distinct}}^{--}$ is due to the fact that increasing N leads to more anions being covalently bound and thus constrained to move together, a phenomenon which will be general to any polyelectrolyte regardless of the chemical properties of the polymer or solvent. The sum of the self- and distinct terms, that is, the overall L^{--}, increases with respect to chain length (Figure S1), corresponding to a decreasing cation transference number.

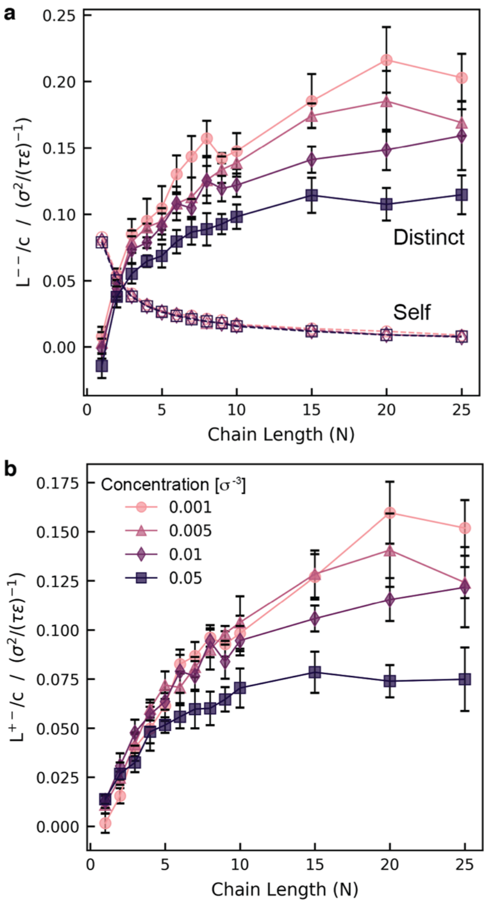

Figure 3. Comparison of anion transport coefficients for each concentration and chain length. (a) L_{self}^{--} (dashed lines) and $L_{\mathrm{distinct}}^{--}$ (solid lines), all divided by concentration to give the contributions to each transport coefficient per ion. (b) L^{+-} divided by concentration.

In addition to the trend with respect to chain length, we also note that t_+ increases with concentration, similar to the previous results obtained with all-atom simulations on PAGELS in DMSO.[16] This can be most clearly understood in terms of cation−anion correlations, as quantified in Figure 3b. The contribution to L^{+-} per ion decreases as the concentration increases, yielding higher t_+ for more concentrated solutions. In order to rationalize the trend of decreasing cation−anion correlations as concentration increases, let us consider the ion pairing behavior of the solutions. Ion pairing is conventionally defined based on a structural analysis of the solution: a cation is considered to be paired at a given time if it is within some specific distance of an anion. The fraction of cations in ion pairs or larger aggregates based on this type of analysis is given in Figure 4a. The resulting trend that ion

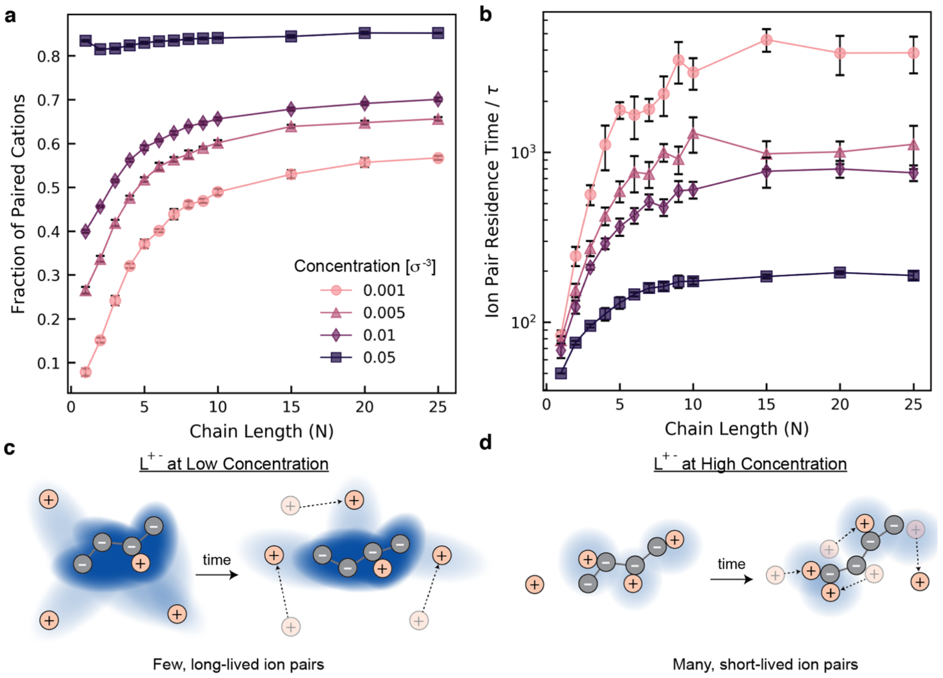

Figure 4. Ion pairing analysis. (a) Fraction of cations in ion pairs or aggregates based on static structural analysis. (b) Ion pair residence times. (c,d) Schematic illustration of cation–anion correlations (L^{+-}) at low (c) and high (d) concentrations. Ion correlations are depicted according to the colormap in Figure 1.

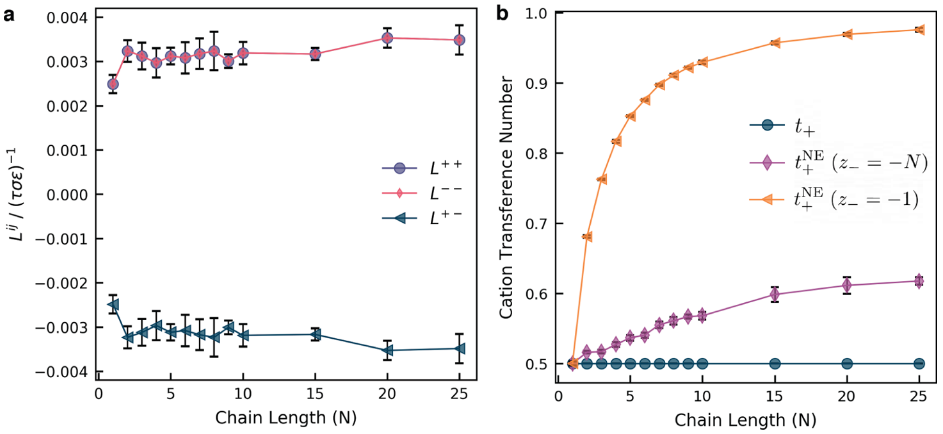

Figure 5. Transport data for the solvent-free solution. (a) Transport coefficients as a function of chain length. The markers for L^{++} and L^{--} directly overlap. (b) Transference number as a function of chain length, computed rigorously (t_+) and using the NE approximation (t_+^{NE}).

pairing increases with concentration, however, is not consistent with the trend of decreasing L^{+-}/c with concentration, suggesting that this static structural analysis does not provide a meaningful assessment of ion correlations in the system. Instead, the trends in L^{+-}/c must be understood with a dynamic analysis of ion pairing, as shown in Figure 4b. Here, we quantify the ion pair residence time, or the characteristic time for an ion pair to exist before breaking apart.[31−33] Despite the fact that more ions are paired at high concentrations, each of these pairs has a shorter lifetime, resulting in overall less correlated cation–anion motion and higher cation transference number. This phenomenon is illustrated schematically in Figure 4c,d. The negative correlation between static ion pairing fraction and dynamic ion pair lifetime was similarly observed in MD simulations of PAGELS in DMSO,[16] suggesting that this may be a common phenomenon in polyelectrolyte solutions.

The lowest concentrations studied yield negative t_+ at high chain lengths. This phenomenon corresponds to the presence of negatively charged aggregates which contribute substantially to the conductivity. For example, if a single cation is bound to a polyanion chain to yield an aggregate with a large negative charge, upon application of an electric field that bound cation will move along with the polymer toward a higher electric potential (in the "wrong direction"). As these negatively charged aggregates are a natural occurrence in polyelectrolytes, it is unsurprising that we observe $t_+ < 0$ (or equivalently $t_- > 1$) for cases at low concentrations when ion pairs are long-lived. In fact, solutions with $t_- > 1$ have been widely reported experimentally for dilute, aqueous polyelectrolytes.[34−38]

Solvent-Free Systems. Given the trend of increasing cation transference number with concentration, the question naturally arises as to whether further increasing concentration may yield polyelectrolytes with t_+ greater than that of the monomeric solution. We can answer this question by considering the limit of a solvent-free system, that is, a polymerized ionic liquid.

We must first revisit our theoretical framework for the case of a solvent-free system. As mentioned above, a system with n components will have $n(n-1)/2$ independent transport coefficients. A two-component electrolyte will thus only have one independent transport coefficient. We remind the reader that $\sum_i M_i L^{ij} = 0$ as a consequence of our center-of-mass reference frame, where M_i is the molar mass of species i. Noting that the masses of all species in our system are equivalent, we can conclude that $L^{++} = L^{--} = -L^{+-}$ in these solvent-free systems. Indeed, the computed transport coefficients follow exactly this relation (Figure 5a; self- and distinct transport coefficients for these systems are provided in Figure S11). The implications of these data are twofold. First, L^{+-} is necessarily negative in a two-component electrolyte, suggesting anticorrelated cation−anion motion. This phenomenon has been previously noted in the ionic liquid literature.[18,39,40] Second, from eq 11, it can be shown that the transference number of these solvent-free solutions is determined solely by the ion charges and masses: $t_+ = z_+M_-/(z_+M_- - z_-M_+)$. This phenomenon, too, has been noted previously for polymerized ionic liquids[18] and molten salts.[41,42] In the polyelectrolyte solutions modeled here, where the cation and monomer masses are the same, $t_+ = 0.5$ for all chain lengths (Figure 5b). In most physically relevant polymerized ionic liquids or single-ion conductors, however, the cation and anion ratios are drastically different. In the polystyrene-TFSI-based systems commonly investigated experimentally,[4,43] for example, the anionic monomer has a molar mass of 314.28 g/mol, compared to the Li-ion mass of 6.94 g/mol. This mass discrepancy would translate to a transference number of 0.98 in a two-component solution of dry lithiated polystyrene-TFSI—in line with the experimental characterization of these types of systems having very high t_+.[4,43] It is important to note that the main utility of the transference number is in dictating the extent of concentration gradients in an electrolyte, which limit a battery's rate capability.[3] As electroneutrality dictates that no concentration gradients may be formed in a solvent-free electrolyte, however, the transference number of these systems is of little physical relevance in predicting battery performance. Regardless, even in this super-concentrated limit, we do not observe any polyelectrolyte solutions with a cation transference number greater than the conventional monomeric systems.

CONCLUSIONS

In this work, we have computed the Onsager transport coefficients in polyelectrolyte solutions as a function of chain length and concentration using coarse-grained molecular dynamics simulations with an explicit solvent. These transport coefficients provide insights into the ion correlations dictating ion motion and allow us to rigorously compute the transference number of the solutions. We demonstrate that the intrinsic anion−anion correlations within the chains result in decreasing t_+ as the chain length increases and cause substantial deviation between the true t_+ and the ideal solution quantity t_+^{NE}. Furthermore, the decrease in t_+ with decreasing concentration can be attributed to stronger cation−anion correlations for more dilute solutions. These stronger correlations are primarily attributed to the longer lifetime of existing ion pairs rather than an increased quantity of ion pairs (defined based on a structural picture of the solution). Even in the case of a solvent-free system (polymerized ionic liquid), we do not observe any polyelectrolyte solutions with a transference number greater than that of a conventional monomeric electrolyte. These results suggest that unentangled, short-chain polyelectrolyte solutions may not be useful as high t_+ alternatives to conventional LIB electrolytes. It is possible that polyelectrolyte solutions or gel-like single-ion conductors may be able to attain a high cation transference number, if the chains are entangled or cross-linked such that the polymer is effectively immobile. Based on eq 3, we see that if the flux of the anion is zero, then L^{--} and L^{+-} will also tend to zero, in which case the transference number would approach unity. While these systems could have a high transference number, these approaches typically yield very low conductivity.[4,6] Thus, there exists a trade-off between the cation transference number and conductivity, which must be resolved in order to achieve promising single-ion conductors.

METHODS

Coarse-Grained Polyelectrolyte Model. Polyanions were represented by the Kremer−Grest bead−spring chain model.[26,27] Adjacent beads, each representing one monomer, interacted via finitely extensible nonlinear elastic (FENE) bonds, where interaction energies take the form

$$U_{\mathrm{FENE}}(r) = -0.5KR_0^{\,2}\ln\left[1-\left(\frac{r}{R_0}\right)^2\right] \tag{14}$$

Here, r is the distance between two monomers, the spring constant $K = 30\varepsilon/\sigma^2$, and the maximum extension of the bond $R_0 = 1.5\ \sigma$. These bonding parameters yield an average bond length of 0.97 σ and avoid unphysical crossing of bonds.[44,45]

Counter ions and solvent molecules were modeled explicitly as charged and neutral beads, respectively. Although it increases the computational cost of the simulations, including the explicit solvent has been shown in several works to be crucial for accurately capturing dynamics in the solution.[46−48] All particles (monomers, cations, and solvent) were subject to a truncated-shifted Lennard-Jones (LJ) potential to account for the excluded volume

$$U_{\mathrm{LJ}}(r) = \begin{cases} 4\varepsilon_{\mathrm{LJ}}\left[\left(\dfrac{\sigma_{\mathrm{LJ}}}{r}\right)^{12} - \left(\dfrac{\sigma_{\mathrm{LJ}}}{r}\right)^{6} - \left(\dfrac{\sigma_{\mathrm{LJ}}}{r_{\mathrm{cut}}}\right)^{12} + \left(\dfrac{\sigma_{\mathrm{LJ}}}{r_{\mathrm{cut}}}\right)^{6}\right] & r \le r_{\mathrm{cut}} \\ 0 & r > r_{\mathrm{cut}} \end{cases} \tag{15}$$

For all interactions, $\varepsilon_{\mathrm{LJ}} = \varepsilon$ (the LJ unit of energy) and $\sigma_{\mathrm{LJ}} = \sigma$, where σ is the LJ unit of distance and the diameter of each of the beads in the system. We choose $r_{\mathrm{cut}} = 2^{1/6}\ \sigma$, which yields good solvent conditions.[49] All species are given unit mass.

Cations and (poly)anions were additionally subject to the Coulomb potential

$$U_{\mathrm{Coulomb}}(r) = \frac{z_i z_j e^2}{4\pi\varepsilon_0\varepsilon_r r} = k_{\mathrm{B}}T\frac{l_{\mathrm{B}} z_i z_j}{r} \tag{16}$$

where e is the elementary charge, ε_0 is the vacuum permittivity, ε_r is the dielectric constant of the medium, and z_i is the charge of species i. Each cation was assigned $z_+ = +1$ and each monomer was given $z_- = -1$. The quantity $l_{\mathrm{B}} = e^2/(4\pi\varepsilon_0\varepsilon_r k_{\mathrm{B}}T)$ is the Bjerrum length, which defines the length scale at which the energy of electrostatic interactions is equal to the thermal energy, $k_{\mathrm{B}}T$. As the simulations in this work capture a wide range of polymer concentrations (from the semi-dilute regime to the limit of a solvent-free system), the dielectric constant was varied linearly as a function of the fraction of the solvent.[50] The lower limit of the dielectric constant, corresponding to a system with only solvent, was chosen to mimic the dielectric properties of water with a Bjerrum length of 7.1 Å. We follow the common procedure[47,49] of mapping the average distance between polymer beads, 0.97 σ, to the size of a polystyrene sulfonate monomer, 2.5 Å, which yields a Bjerrum length of $l_B = 7.1$ Å × (0.97 σ/2.5 Å) = 2.75 σ. The upper limit of the Bjerrum length for the system with no solvent was chosen to be 30 σ, in the range commonly chosen to study melts of charged polymers.[29,44]

Note that with the length scale mapping of 2.5 Å ≈ 0.97 σ, the ion concentrations simulated in this work (0.001, 0.005, 0.01, and 0.05 σ^{-3}) can be roughly mapped to concentrations of 0.1, 0.48, 0.97, and 4.8 M.

Simulation Details. Polymer chains were initially prepared using a self-avoiding random walk. The polymers, cations, and solvent particles were randomly packed into a cubic simulation box using PACKMOL[51] at a density of 0.8 σ^{-3}, a value in the range commonly used to study both dilute polyelectrolyte solutions as well as polymer melts.[29,44,52−55] With the exception of the systems at the lowest concentration studied, 0.001 σ^{-3}, each simulation consisted of approximately 40,000 particles, with the exact number varied slightly to precisely reach the target concentration. It was verified that doubling the number of particles in the simulation box did not have any appreciable effect on the computed transport properties. At 0.001 σ^{-3}, however, finite size effects were more pronounced because of the smaller number of polymer chains in the system and the larger charge screening length. Simulations at this concentration were run with 80,000 particles, with one run using 120,000 particles to verify that there were no appreciable finite size effects with this larger box size. The systems with the longest chain length ($N = 25$) had 4, 10, 20, and 100 polymer chains for concentrations of 0.001, 0.005, 0.01, and 0.05 σ^{-3}, respectively.

MD simulations were performed using the LAMMPS code.[56,57] The as-prepared system was equilibrated using a conjugate gradient energy minimization. Simulations were run for a total of 10^7 steps, with a time step of 0.005 τ. The first 4×10^5 steps (2000 τ) were considered to be an equilibration period and not used for data analysis. This equilibration period was long enough for the polymer end-to-end vector autocorrelation function to decay to less than 0.1 for all systems (Figure S12), suggesting that there were minimal effects of the initial system configuration by the time data collection began. We further confirmed that the polymers' radii of gyration and the total system energy had stabilized by the end of the equilibration period.

The equations of motion were numerically integrated using the velocity-Verlet algorithm, with periodic boundary conditions in all three spatial directions. A Nosé−Hoover style thermostat was used to maintain the temperature of the system at $k_BT/\varepsilon = 1$. Long-range Coulombic interactions were evaluated using the PPPM method.[58]

Data Analysis. Transport coefficients were computed using eq 4

$$L^{ij} = \frac{1}{6k_BTV}\lim_{t\to\infty}\frac{\mathrm{d}}{\mathrm{d}t}\left\langle \sum_{\alpha}[\boldsymbol{r}_i^{\alpha}(t) - \boldsymbol{r}_i^{\alpha}(0)]\cdot\sum_{\beta}[\boldsymbol{r}_j^{\beta}(t) - \boldsymbol{r}_j^{\beta}(0)]\right\rangle$$

The angular brackets denote averaging over all time origins within the trajectory. The self-terms L^{ii}_{self} (and thus the diffusion coefficients, by eq 8) are computed in an analogous manner using eq 6, and the distinct terms were computed by $L^{ii}_{\mathrm{distinct}} = L^{ii} - L^{ii}_{\mathrm{self}}$. All experimentally relevant quantities such as the transference number are computed from L^{ij} using eqs 9−11.

In order to capture true diffusive transport, the term in angular brackets of eqs 4 or 6 must be linear with respect to time, that is, $\langle\sum_{\alpha}[\boldsymbol{r}_i^{\alpha}(t) - \boldsymbol{r}_i^{\alpha}(0)]\cdot\sum_{\beta}[\boldsymbol{r}_j^{\beta}(t) - \boldsymbol{r}_j^{\beta}(0)]\rangle \propto t^{\beta}$ and $\sum_{\alpha}\langle[\boldsymbol{r}_i^{\alpha}(t) - \boldsymbol{r}_i^{\alpha}(0)]^2\rangle \propto t^{\beta}$, with $\beta = 1$. For most simulations in this work, β was computed to be between 0.94 and 1.05, with analysis performed over at least a decade of time. This suggests that the simulations have been run long enough to reach and adequately sample the diffusive regime. Representative data demonstrating this linear behavior is given in Figure S4. There are a two classes of exceptions in which β deviates more substantially from unity. The first is for L^{+-} in the monomer simulations ($N = 1$) at the three lowest concentrations studied, in which case β became as low as 0.84. This deviation from linearity is because of the small overall magnitude of L^{+-}, which results in more noise in the fitting procedure. As $L^{+-} \approx 0$ for these systems, the fact that we do not observe linear behavior does not impact any of our conclusions. The second case where β departs from unity is for L^{--}_{self} in the solvent-free systems for chain lengths of 15, 20, and 25, where β reached as low as 0.73. This sub-diffusive behavior can be attributed to anion motion corresponding to intrachain degrees of freedom, such as chain rotations. While the values of L^{--}_{self} for these three chain lengths, as presented in Figure S11, cannot be rigorously interpreted as transport coefficients because of this deviation from linearity, this does not affect any of the conclusions drawn in this work.

The extent of ion pairing, as shown in Figure 4a, is evaluated using a distance criterion: all cations within a given cutoff distance of any anion were considered paired. This cutoff distance was chosen as the first minimum of the cation−anion radial distribution function (1.6 σ, see Figure S14), which was consistent across all chain lengths and concentrations. The residence times of ion pairs, as shown in Figure 4b, are evaluated by computing the lifetime correlation function $P_{\alpha\beta}(t) = \langle H_{\alpha\beta}(t)H_{\alpha\beta}(0)\rangle$, where $H_{\alpha\beta}(t)$ is one if particles α and β are neighbors at time t and zero otherwise.[16,31−33] Two particles are deemed neighbors if they fall within a distance cutoff, chosen based on the radial distribution function to be 2.5 σ to coincide with the minimum after the second solvation shell of the ions. This distance cutoff was larger than that used for the static evaluation of ion pairing, as we observed that ions moved very frequently back and forth between the first and second solvation shells. The residence time was defined as the time for $P_{\alpha\beta}(t)$ to decay to 10% of its original value.

Error bars throughout this text are given as the standard deviation of five independent replicates. Trajectories were analyzed using an in-house code which utilized the Python package MDAnalysis.[59,60] Code is available at https://github.com/kdfong/transport-coefficients-MSD.

No unexpected or unusually high safety hazards were encountered.

■ ASSOCIATED CONTENT

Supporting Information

The Supporting Information is available free of charge at https://pubs.acs.org/doi/10.1021/acs.macromol.0c02001.

Additional transport coefficient data and discussion; conductivity, mobility, and diffusion coefficients; characterization of polymer size and relaxation time; and radial distribution functions (PDF)

■ AUTHOR INFORMATION

Corresponding Authors

Bryan D. McCloskey − *Department of Chemical and Biomolecular Engineering, University of California Berkeley, Berkeley, California 94720-1900, United States; Energy Technologies Area, Lawrence Berkeley National Laboratory, Berkeley, California 94720, United States;* orcid.org/0000-0001-6599-2336; Email: bmcclosk@berkeley.edu

Kristin A. Persson − *Department of Materials Science and Engineering, University of California Berkeley, Berkeley, California 94720-1900, United States; Energy Technologies Area, Lawrence Berkeley National Laboratory, Berkeley, California 94720, United States;* orcid.org/0000-0003-2495-5509; Email: kapersson@lbl.gov

Authors

Kara D. Fong − *Department of Chemical and Biomolecular Engineering, University of California Berkeley, Berkeley, California 94720-1900, United States; Energy Technologies Area, Lawrence Berkeley National Laboratory, Berkeley,* *California 94720, United States;* orcid.org/0000-0002-0711-097X

Julian Self − *Department of Materials Science and Engineering, University of California Berkeley, Berkeley, California 94720-1900, United States; Energy Technologies Area, Lawrence Berkeley National Laboratory, Berkeley, California 94720, United States;* orcid.org/0000-0002-5486-9559

Complete contact information is available at:
https://pubs.acs.org/10.1021/acs.macromol.0c02001

Notes

The authors declare no competing financial interest.

■ ACKNOWLEDGMENTS

The authors would like to thank Kranthi K. Mandadapu for insightful feedback and guidance on the theory discussed herein, as well as Helen K. Bergstrom and Kyle M. Diederichsen for helpful discussions on polyelectrolyte transport. K.D.F. acknowledges support from NSF GRFP under grant no. DGE 1752814. This work was supported by the Assistant Secretary for Energy Efficiency and Renewable Energy, Vehicle Technologies Office, of the U.S. Department of Energy under Contract DE-AC02-05CH11231, under the Advanced Battery Materials Research (BMR) Program managed by Tien Duong. This research used resources of the Savio computational cluster resource provided by the Berkeley Research Computing program at the University of California, Berkeley (supported by the UC Berkeley Chancellor, Vice Chancellor for Research, and Chief Information Officer).

■ REFERENCES

(1) Doyle, M.; Fuller, T. F.; Newman, J. The importance of the lithium ion transference number in lithium/polymer cells. *Electrochim. Acta* **1994**, *39*, 2073−2081.

(2) Newman, J.; Thomas-Alyea, K. E. *Electrochemical Systems*, 3rd ed.; John Wiley & Sons, Inc., 2004.

(3) Diederichsen, K. M.; McShane, E. J.; McCloskey, B. D. Promising routes to a high Li^+ transference number electrolyte for lithium ion batteries. *ACS Energy Lett.* **2017**, *2*, 2563−2575.

(4) Zhang, H.; Li, C.; Piszcz, M.; Coya, E.; Rojo, T.; Rodriguez-Martinez, L. M.; Armand, M.; Zhou, Z. Single lithium-ion conducting solid polymer electrolytes: Advances and perspectives. *Chem. Soc. Rev.* **2017**, *46*, 797−815.

(5) Jeong, K.; Park, S.; Lee, S.-Y. Revisiting polymeric single lithium-ion conductors as an organic route for all-solid-state lithium ion and metal batteries. *J. Mater. Chem. A* **2019**, *7*, 1917−1935.

(6) Bocharova, V.; Sokolov, A. P. Perspectives for polymer electrolytes: A view from fundamentals of ionic conductivity. *Macromolecules* **2020**, *53*, 4141−4157.

(7) Strauss, E.; Menkin, S.; Golodnitsky, D. On the way to high-conductivity single lithium-ion conductors. *J. Solid State Electrochem.* **2017**, *21*, 1879−1905.

(8) Kreuer, K.-D.; Wohlfarth, A.; De Araujo, C. C.; Fuchs, A.; Maier, J. Single alkaline-ion (Li^+, Na^+) conductors by ion exchange of proton-conducting ionomers and polyelectrolytes. *ChemPhysChem* **2011**, *12*, 2558−2560.

(9) Smiatek, J.; Wohlfarth, A.; Holm, C. The solvation and ion condensation properties for sulfonated polyelectrolytes in different solvents - A computational study. *New J. Phys.* **2014**, *16*, 025001.

(10) Buss, H. G.; Chan, S. Y.; Lynd, N. A.; McCloskey, B. D. Nonaqueous polyelectrolyte solutions as liquid electrolytes with high lithium ion transference number and conductivity. *ACS Energy Lett.* **2017**, *2*, 481−487.

(11) Diederichsen, K. M.; Fong, K. D.; Terrell, R. C.; Persson, K. A.; McCloskey, B. D. Investigation of solvent type and salt addition in high transference number nonaqueous polyelectrolyte solutions for lithium ion batteries. *Macromolecules* **2018**, *51*, 8761−8771.

(12) Diederichsen, K. M.; Terrell, R. C.; McCloskey, B. D. Counterion transport and transference number in aqueous and nonaqueous short-chain polyelectrolyte solutions. *J. Phys. Chem. B* **2019**, *123*, 10858−10867.

(13) Diederichsen, K. M.; McCloskey, B. D. Electrolyte additives to enable nonaqueous polyelectrolyte solutions for lithium ion batteries. *Mol. Syst. Des. Eng.* **2020**, *5*, 91−96.

(14) Dewing, B. L.; Bible, N. G.; Ellison, C. J.; Mahanthappa, M. K. Electrochemically stable, high transference number lithium bis(malonato) borate polymer solution electrolytes. *Chem. Mater.* **2020**, *32*, 3794−3804.

(15) Valøen, L. O.; Reimers, J. N. Transport properties of $LiPF_6$-based Li-ion battery electrolytes. *J. Electrochem. Soc.* **2005**, *152*, A882.

(16) Fong, K. D.; Self, J.; Diederichsen, K. M.; Wood, B. M.; McCloskey, B. D.; Persson, K. A. Ion transport and the true transference number in nonaqueous polyelectrolyte solutions for lithium ion batteries. *ACS Cent. Sci.* **2019**, *5*, 1250−1260.

(17) Qian, W.; Texter, J.; Yan, F. Frontiers in poly(ionic liquid)s: Syntheses and applications. *Chem. Soc. Rev.* **2017**, *46*, 1124−1159.

(18) Zhang, Z.; Wheatle, B. K.; Krajniak, J.; Keith, J. R.; Ganesan, V. Ion mobilities, transference numbers, and inverse Haven ratios of polymeric ionic liquids. *ACS Macro Lett.* **2019**, *9*, 84−89.

(19) Yu, Y.; Lu, F.; Sun, N.; Wu, A.; Pan, W.; Zheng, L. Single lithium-ion polymer electrolytes based on poly(ionic liquid)s for lithium-ion batteries. *Soft Matter* **2018**, *14*, 6313−6319.

(20) Kisliuk, A.; Bocharova, V.; Popov, I.; Gainaru, C.; Sokolov, A. P. Fundamental parameters governing ion conductivity in polymer electrolytes. *Electrochim. Acta* **2019**, *299*, 191−196.

(21) Gainaru, C.; Stacy, E. W.; Bocharova, V.; Gobet, M.; Holt, A. P.; Saito, T.; Greenbaum, S.; Sokolov, A. P. Mechanism of conductivity relaxation in liquid and polymeric electrolytes: Direct link between conductivity and diffusivity. *J. Phys. Chem. B* **2016**, *120*, 11074−11083.

(22) Muthukumar, M. 50th Anniversary perspective: A perspective on polyelectrolyte solutions. *Macromolecules* **2017**, *50*, 9528−9560.

(23) Dobrynin, A. V. *Polymer Science: A Comprehensive Reference*, 10 Volume Set; Elsevier, 2012; Vol. *1*; pp 81−132.

(24) Fong, K. D.; Bergstrom, H. K.; McCloskey, B. D.; Mandadapu, K. K. Transport phenomena in electrolyte solutions: Non-equilibrium thermodynamics and statistical mechanics. **2020**, arXiv:2006.16164. arXiv preprint.

(25) Bird, R. B.; Klingenberg, D. J. Multicomponent diffusion—A brief review. *Adv. Water Resour.* **2013**, *62*, 238−242.

(26) Kremer, K.; Grest, G. S. Dynamics of entangled linear polymer melts: A molecular-dynamics simulation. *J. Chem. Phys.* **1990**, *92*, 5057−5086.

(27) Grest, G. S.; Kremer, K. Molecular dynamics simulation for polymers in the presence of a heat bath. *Phys. Rev. A* **1986**, *33*, 3628.

(28) Hoy, R. S.; Foteinopoulou, K.; Kröger, M. Topological analysis of polymeric melts: Chain-length effects and fast-converging estimators for entanglement length. *Phys. Rev. E: Stat., Nonlinear, Soft Matter Phys.* **2009**, *80*, 031803.

(29) Hall, L. M.; Seitz, M. E.; Winey, K. I.; Opper, K. L.; Wagener, K. B.; Stevens, M. J.; Frischknecht, A. L. Ionic aggregate structure in ionomer melts: Effect of molecular architecture on aggregates and the ionomer peak. *J. Am. Chem. Soc.* **2012**, *134*, 574−587.

(30) Nyquist, R. M.; Ha, B.-Y.; Liu, A. J. Counterion condensation in solutions of rigid polyelectrolytes. *Macromolecules* **1999**, *32*, 3481−3487.

(31) Self, J.; Fong, K. D.; Persson, K. A. Transport in super-concentrated $LiPF_6$ and $LiBF_4$/propylene carbonate electrolytes. *ACS Energy Lett.* **2019**, *4*, 2843−2849.

(32) Solano, C. J. F.; Jeremias, S.; Paillard, E.; Beljonne, D.; Lazzaroni, R. A joint theoretical/experimental study of the structure,

dynamics, and Li^+ transport in bis([tri]fluoro[methane]sulfonyl)-imide [T] FSI-based ionic liquids. *J. Chem. Phys.* **2013**, *139*, 034502.

(33) Borodin, O.; Smith, G. D.; Henderson, W. Li^+ cation environment, transport, and mechanical properties of the LiTFSI doped N-methyl-N-alkylpyrrolidinium$^+$TFSI$^-$ ionic liquids. *J. Phys. Chem. B* **2006**, *110*, 16879−16886.

(34) Joshi, Y. M.; Kwak, J. C.T. Transference numbers, polyion mobilities, and charge fractions in aqueous solutions of lithium, sodium, and potassium dextransulfate. *Biophys. Chem.* **1980**, *12*, 323−328.

(35) Jordan, D. O.; Kurucsev, T.; Martin, M. L. Comparative physical chemical study of isotactic and atactic poly (styrene sulphonic acid) solutions. Part 2. Electrical conductance and transference measurements in salt-free aqueous solutions. *Trans. Faraday Soc.* **1969**, *65*, 606−611.

(36) De, R.; Lee, H.; Das, B. Exploring the interactions in binary mixtures of polyelectrolytes: Influence of mixture composition, concentration, and temperature on counterion condensation. *J. Mol. Liq.* **2018**, *251*, 94−99.

(37) Kuznetsov, I. A.; Vorontsova, O. V.; Kozlov, A. G. Polyelectrolyte properties of biopolymers: Conductivity and secondary structure of polyriboadenylic acid and its salts in solutions. *Biopolymers* **1991**, *31*, 65−76.

(38) Overbeek, J. T. G. *Macromolecular Chemistry-11*; Elsevier, 1977; pp 91−101.

(39) Kashyap, H. K.; Annapureddy, H. V. R.; Raineri, F. O.; Margulis, C. J. How is charge transport different in ionic liquids and electrolyte solutions? *J. Phys. Chem. B* **2011**, *115*, 13212−13221.

(40) McDaniel, J. G.; Son, C. Y. Ion correlation and collective dynamics in BMIM/BF_4-based organic electrolytes: From dilute solutions to the ionic liquid limit. *J. Phys. Chem. B* **2018**, *122*, 7154−7169.

(41) Matsunaga, S.; Koishi, T.; Tamaki, S. Velocity correlation functions and partial conductivities of molten AgI−AgBr by molecular dynamics simulation. *J. Mater. Sci. Eng. A* **2007**, *449−451*, 693−698.

(42) Koishi, T.; Tamaki, S. Partial conductivities of a molten salt based on Langevin equation. *J. Phys. Soc. Jpn.* **1999**, *68*, 964−971.

(43) Bouchet, R.; Maria, S.; Meziane, R.; Aboulaich, A.; Lienafa, L.; Bonnet, J.-P.; Phan, T. N. T.; Bertin, D.; Gigmes, D.; Devaux, D.; et al. Single-ion BAB triblock copolymers as highly efficient electrolytes for lithium-metal batteries. *Nat. Mater.* **2013**, *12*, 452−457.

(44) Ma, B.; Nguyen, T. D.; Olvera de la Cruz, M. Control of ionic mobility via charge size asymmetry in random ionomers. *Nano Lett.* **2019**, *20*, 43−49.

(45) Chang, R.; Yethiraj, A. Strongly charged flexible polyelectrolytes in poor solvents: Molecular dynamics simulations with explicit solvent. *J. Chem. Phys.* **2003**, *118*, 6634−6647.

(46) Yao, N.; Li, J.; Gu, F.; Wang, H.; Liao, Q. Relaxation time spectrum and dynamics of stretched polymer chain in dilute θ solution: Implicit solvent model versus explicit solvent model. *Macromol. Theory Simul.* **2020**, *29*, 1900064.

(47) Grass, K.; Holm, C. Polyelectrolytes in electric fields: Measuring the dynamical effective charge and effective friction. *Soft Matter* **2009**, *5*, 2079−2092.

(48) Chang, R.; Yethiraj, A. Dilute solutions of strongly charged flexible polyelectrolytes in poor solvents: Molecular dynamics simulations with explicit solvent. *Macromolecules* **2006**, *39*, 821−828.

(49) Micka, U.; Holm, C.; Kremer, K. Strongly charged, flexible polyelectrolytes in poor solvents: Molecular dynamics simulations. *Langmuir* **1999**, *15*, 4033−4044.

(50) Hall, D. S.; Self, J.; Dahn, J. R. Dielectric constants for quantum chemistry and Li-ion batteries: Solvent blends of ethylene carbonate and ethyl methyl carbonate. *J. Phys. Chem. C* **2015**, *119*, 22322−22330.

(51) Martínez, L.; Andrade, R.; Birgin, E. G.; Martínez, J. M. PACKMOL: A package for building initial configurations for molecular dynamics simulations. *J. Comput. Chem.* **2009**, *30*, 2157−2164.

(52) Lo, T. S.; Khusid, B.; Koplik, J. Dynamical clustering of counterions on flexible polyelectrolytes. *Phys. Rev. Lett.* **2008**, *100*, 128301.

(53) Chremos, A.; Douglas, J. F. Counter-ion distribution around flexible polyelectrolytes having different molecular architecture. *Soft Matter* **2016**, *12*, 2932−2941.

(54) Carrillo, J.-M. Y.; Brown, W. M.; Dobrynin, A. V. Explicit solvent simulations of friction between brush layers of charged and neutral bottle-brush macromolecules. *Macromolecules* **2012**, *45*, 8880−8891.

(55) Hall, L. M.; Stevens, M. J.; Frischknecht, A. L. Dynamics of model ionomer melts of various architectures. *Macromolecules* **2012**, *45*, 8097−8108.

(56) Plimpton, S. Fast parallel algorithms for short-range molecular dynamics. *J. Comput. Phys.* **1995**, *117*, 1−19.

(57) http://lammps.sandia.gov (accessed Aug 11, 2017).

(58) Toukmaji, A. Y.; Board, J. A. Ewald summation techniques in perspective: A survey. *Comput. Phys. Commun.* **2003**, *95*, 73−92.

(59) Michaud-Agrawal, N.; Denning, E. J.; Woolf, T. B.; Beckstein, O. MDAnalysis: A toolkit for the analysis of molecular dynamics simulations. *J. Comput. Chem.* **2011**, *32*, 2319−2327.

(60) Gowers, R.; Linke, M.; Barnoud, J.; Reddy, T.; Melo, M.; Seyler, S.; Domański, J.; Dotson, D.; Buchoux, S.; Kenney, I.; Beckstein, O. MDAnalysis: A Python package for the rapid analysis of molecular dynamics simulations. *Proceedings of the 15th Python in Science Conference*, 2016; pp 98−105.

https://dx.doi.org/10.1021/acs.macromol.0c02001
Macromolecules XXXX, XXX, XXX−XXX